Z. Kristallogr. Suppl. **26** (2007) 423-428

Time-resolved synchrotron X-ray powder diffraction study of biogenic nano-magnetite

A.M.T. Bell[1*], V.S. Coker[2], C.I. Pearce[2],R.A.D. Pattrick[2], G. van der Laan[1,2] and J.R. Lloyd[2]

[1] CCLRC Daresbury Laboratory, Daresbury, Warrington, WA4 4AD, UK.
[2] School of Earth, Atmospheric and Environmental Sciences, The University of Manchester, Oxford Road, Manchester, M13 9PL, UK.
[*]a.m.t.bell@dl.ac.uk

Keywords: powder diffraction, iron oxides, synchrotron radiation, biotransformation.

Abstract. The bacterium *Geobacter sulfurreducens* can produce nanoparticulate magnetite (Fe_3O_4) by the reduction of amorphous Fe(III) oxyhydroxide coupled to the oxidation of organic matter in the anoxic subsurface as an alternative to oxygen respiration. *G. sulfurreducens* can transfer electrons to solid Fe(III)-bearing minerals through either direct contact between the cell and the mineral surface or by using an electron shuttling compound. High-resolution synchrotron X-ray powder diffraction has been used to study samples taken at different stages of this reaction. This shows that an initial amorphous phase first transforms to goethite (FeO(OH)), before undergoing a further transformation to magnetite. Magnetite is formed faster in the presence of the electron shuttling compound disodium anthraquinone 2,6 disulphonate.

Introduction

The bacterium *Geobacter sulfurreducens* can produce nanoparticulate magnetite (Fe_3O_4) by the reduction of amorphous Fe(III) oxyhydroxide coupled to the oxidation of organic matter in the anoxic subsurface as an alternative to oxygen respiration. Nanoparticulate goethite (FeO(OH)) is formed as an intermediate phase. *G. sulfurreducens* can transfer electrons to solid Fe(III)-bearing minerals through either direct contact between the cell and the mineral surface or by using an electron shuttling compound. High resolution synchrotron X-ray powder diffraction has been used to study different stages of this biotransformation reaction. In all figures and tables goethite is indicated by **G** and magnetite by **M**.

Experimental

Nanoparticulate iron oxides were prepared [1] by bacterial transformation both with and without the electron shuttling compound anthraquinone 2,6-disulfonate (AQDS). Samples were taken at different stages of this reaction (0, 3, 7, 14, 26, 50, 102, 176 and 2037 hours) and loaded into borosilicate glass capillaries. Data were collected with a synchrotron X-ray wavelength of 0.9Å in capillary mode using the high resolution powder diffractometer on station 2.3 [2,3] of the Daresbury SRS; samples were cooled to 193K using an Oxford Cryosystems Cryostream to prevent sample oxidation.

Data analysis

Analysis of the powder diffraction data showed that both reactions, with and without AQDS, appeared to go through four stages. The first stage was amorphous with no iron oxide phase Bragg reflections present, just two broad "humps" with d-spacings of 2.51 and 1.46 Å. The second stage just showed Bragg reflections due to goethite (FeO(OH) – Pnma orthorhombic). The third stage showed Bragg reflections from a mixture of goethite and magnetite (Fe_3O_4 – Fd3m cubic). The fourth and final stage just showed Bragg reflections due to single-phase magnetite. The reaction proceeded faster for the samples prepared with AQDS (see figure 1) compared to the reaction for the samples prepared without AQDS (see figure 2).

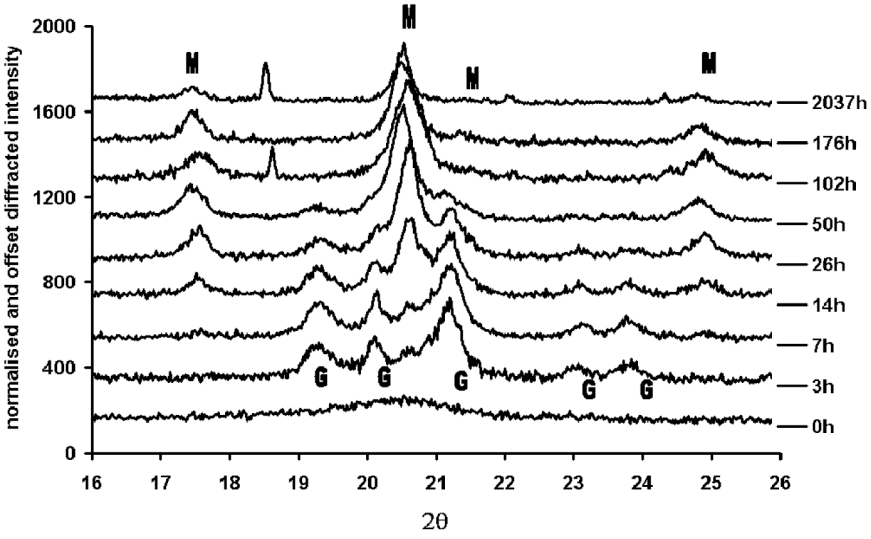

Figure 1. Synchrotron X-ray powder diffraction data for AQDS samples taken at the indicated reaction times. Peaks at ~18.5°2θ in 102h and 2037h data are due to the wax used to mount the capillaries.

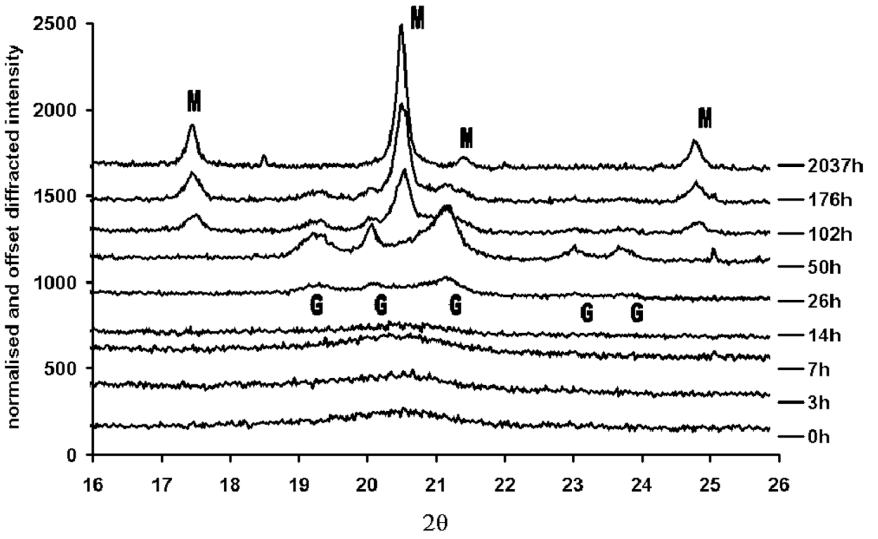

Figure 2. Synchrotron X-ray powder diffraction data for non AQDS samples taken at the indicated reaction times.

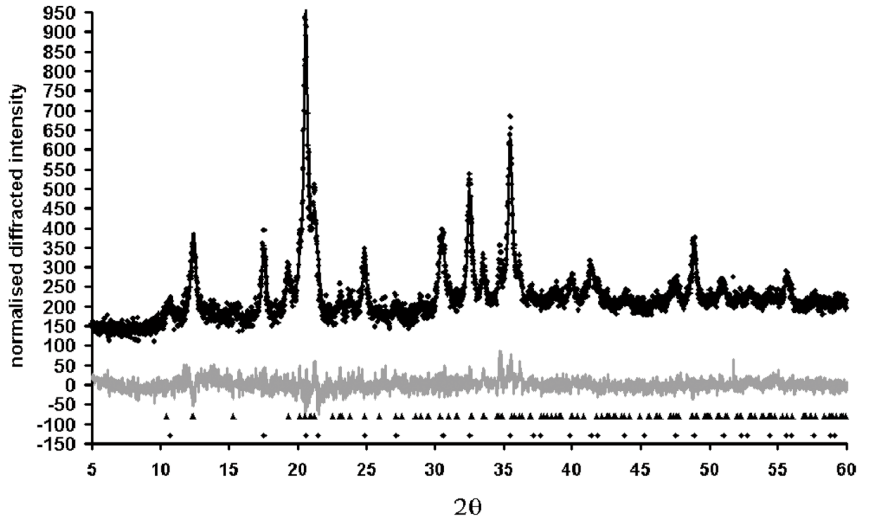

Figure 3. Rietveld plot for AQDS 26h sample Upper and lower tickmarks respectively indicate goethite and magnetite Bragg reflections.

Rietveld refinement

Rietveld [4] refinement was done using the TOPAS [5] software package. Appropriate structural parameters for goethite [6] and magnetite [7] were refined. A Rietveld difference plot for the AQDS 26h is shown as figure 3. Tables 1 (AQDS) and 2 (non-AQDS) show selected refined structural parameters. In these tables errors for these parameters are given for the last 2 significant figures, CS indicates crystallite size.

Table 1. Refined structural parameters for goethite and magnetite for AQDS samples.

Sample	3h	7h	14h	26h	50h
G wt.%	100	87.46(48)	68.35(56)	44.09(62)	26.71(92)
M wt.%	0	12.54(48)	31.65(56)	55.91(62)	73.29(92)
G a(Å)	9.9556(53)	9.9484(32)	9.9586(39)	9.9450(47)	9.9649(67)
G b(Å)	3.0304(15)	3.02659(91)	3.0283(11)	3.0268(14)	3.0353(19)
G c(Å)	4.6259(30)	4.6138(20)	4.6213(23)	4.6101(24)	4.5587(24)
G V(Å^3)	139.56(14)	138.922(85)	139.37(10)	138.77(12)	137.88(15)
G Fe-O1(Å)	1.868(26)	1.925(17)	1.958(23)	1.935(16)	2.048(44)
G Fe-O1(Å)x2	2.013(16)	1.970(10)	1.960(13)	1.972(29)	1.956(26)
G Fe-O2(Å)	2.023(27)	2.077(17)	2.038(24)	2.041(30)	2.048(49)
G Fe-O2(Å)x2	2.214(17)	2.175(11)	2.130(15)	2.151(19)	1.866(28)
G CS (nm)	10.53(61)	12.10(50)	12.58(66)	11.67(63)	#
G strain	0.00(13)	0.000(81)	0.00(10)	0.00(11)	1.53(22)
M a(Å)		8.3766(55)	8.3795(19)	8.3801(13)	8.3808(16)
M O xyz		0.2629(42)	0.2573(16)	0.25481(82)	0.25682(68)
M Fe1-O(Å)x4		2.001(60)	1.920(23)	1.884(12)	1.9135(98)
M Fe2-O(Å)x6		1.992(29)	2.035(11)	2.0555(62)	2.0396(50)
M CS (nm)		7.6(15)	16.7(13)	15.08(54)	18.2(11)
M strain		0.00(50)	0.151(94)	0.017(47)	0.347(78)
Sample	102h	176h	2037h		
G wt.%	0	0	0		
M wt.%	100	100	100		
M a(Å)	8.3799(19)	8.3761(22)	8.3813(40)		
M O xyz	0.25470(87)	0.25438(97)	0.2573(25)		
M Fe1-O(Å)x4	1.883(13)	1.877(14)	1.921(36)		
M Fe2-O(Å)x6	2.0563(67)	2.0580(74)	2.036(18)		
M CS (nm)	11.79(45)	28.8(33)	37(10)		
M strain	0.010(65)	0.597(95)	0.50(17)		

 # The refined goethite crystallite size for this sample is excluded as it is unrealistically large.

Discussion

AQDS samples: The reaction reaches stage 1 after 0h, stage 2 after 3h, stage 3 after 7h and stage 4 after 102h. Table 1 shows some significant differences between lattice parameters and bond lengths for goethite in the 3h to 50h samples. The largest differences appear to be

between the c lattice parameters and some of the Fe-O distances. This suggests that as goethite transforms into magnetite there is a change in the structure of goethite along the crystallographic c-axis. However, for the goethite phase there are no significant differences in crystallite size and this phase is unstrained. Table 1 shows that the magnetite Fe-O distances are significantly different in the 7h sample to that in the other magnetite containing samples. As the reaction proceeds the magnetite Fe-O distances get closer to that in the initial magnetite structure used for refinement [7], by the 102h these distances are the same as the starting structure within error limits. As the reaction progresses the refined crystallite size parameter for magnetite tends to increase. Magnetite in the 14h to 2037h samples is strained but is unstrained in the 7h sample.

Non-AQDS samples: The reaction is slower for the non-AQDS samples. The reaction stays in stage 1 up to 14h, reaches stage 2 after 26h, stage 3 after 50h and doesn't reach stage 4 until 2037h. Table 2 shows that for the non-AQDS samples there are big differences between goethite in the 26h and the 50h to 176h samples. The unit cell volume and crystallite size are much smaller and there are differences in some of the Fe-O distances. The non-AQDS goethite phase is unstrained. Table 2 shows that for the non-AQDS samples the magnetite

Table 2. Refined structural parameters for goethite and magnetite for non-AQDS samples.

Sample	26h	50h	102h	176h	2037h
G wt.%	100	91.76(94)	62.28(87)	38.4(12) *	0
M wt.%	0	8.24(94)	37.72(87)	59.3(11) *	100
G a(Å)	9.903(38)	9.9413(45)	9.9494(59)	9.9590(66)	
G b(Å)	3.024(13)	3.0248(12)	3.0290(17)	3.0311(20)	
G c(Å)	4.467(20)	4.6091(28)	4.6012(29)	4.5858(27)	
G V(Å^3)	133.78(97)	138.60(12)	138.67(14)	138.43(15)	
G Fe-O1(Å)	2.730(26)	1.926(18)	2.022(31)	2.010(47)	
G Fe-O1(Å)x2	1.641(10)	1.965(11)	1.924(17)	1.921(27)	
G Fe-O2(Å)	1.859(40)	2.052(19)	2.005(21)	2.075(53)	
G Fe-O2(Å)x2	2.199(22)	2.126(12)	2.005(35)	1.895(30)	
G CS (nm)	1.96(11)	10.13(44)	10.52(63)	14.4(12)	
G strain	0.00(91)	0.00(11)	0.00(17)	0.00(19)	
M a(Å)		8.393(12)	8.3811(16)	8.3853(12)	8.3857(12)
M O xyz		0.2703(56)	0.2577(11)	0.25663(89)	0.2559(11)
M Fe1-O(Å)x4		2.113(81)	1.927(16)	1.912(13)	1.901(16)
M Fe2-O(Å)x6		1.943(35)	2.0326(82)	2.0422(66)	2.0483(82)
M CS (nm)		6.2(21)	26.0(23)	30.7(25)	52.0(60)
M strain		0.0(10)	0.203(75)	0.200(59)	0.218(52)

** 2.28(25)% ice was present as a 3rd phase due to sample icing in the cryostream.*

phase in the 50h sample is different to that in the 102h to 2037h samples. In the 50h sample the magnetite phase is unstrained and the crystallite size is much smaller than in the 102h to 2037h samples. Also the magnetite O xyz co-ordinates are significantly different in the 50h sample to that in the 102h to 2037h samples. As the non-AQDS reaction is slower it is possible to see very poorly crystalline goethite and magnetite precursor phases, these phases show

some differences to the more crystalline phases which appear later in the reaction. These precursor phases are not seen in the faster AQDS reaction.

Concluding remarks

High-resolution synchrotron X-ray powder diffraction has been used to study reactions where the bacterium *Geobacter Sulfurreducencs* has been used to produce nanoparticulate magnetite from amorphous FeO(OH). The reaction with the presence of the electron shuttling compound anthraquinone 2,6 disulphonate (AQDS) is faster than the reaction without AQDS.
In both reactions an intermediate goethite phase is observed before magnetite. In the slower non-AQDS reaction it is possible to identify very poorly crystalline goethite and magnetite precursor phases.

References

1. Coker, V.S., Bell, A.M.T., Pearce, C.I., Pattrick, R.A.D., van der Laan, G. & Lloyd, J.R., 2006, submitted to *American Mineralogist.*
2. Cernik, R.J., Murray, P.K., Pattison, P. & Fitch, A.N., 1990, *J.Appl. Cryst.*, **23,** 292-296.
3. Collins, S.P., Cernik, R.J., Pattison, P., Bell, A.M.T. & Fitch, A.N., 1992, *Rev. Sci. Instrum.*, **63,** 1013-4.
4. Rietveld, H.M., 1969, *J.Appl. Cryst.*, **2,** 65-71.
5. Coelho, A. A. 2004, TOPAS-Academic.
6. Scheinost, A.C., Stanjek, H., Schulze, D.G. & Gasser, U., 2001, *Amer. Mineral.*, **86(1-2)**, 139-146.
7. Finger, L.W., Hazen, R.M. & Hofmeister, A.M., 1996, *Phys. Chem. Minerals*, **13**, 215-220.

Acknowledgements. We wish to thank CCLRC for award of Daresbury beam time. Vicky Coker wishes to thank EPSRC, CCLRC and Mini-Waste Faraday for a CASE studentship.